

# Subcellular localization of mouse and human UBE3A protein isoforms

S.T. Munshi<sup>1,§</sup>, R.A. Trezza<sup>2,3,4,§</sup>, M. Sonzogni<sup>2,3</sup>, R. Ballarino<sup>1</sup>,  
H. Smeeks<sup>1</sup>, B. Lendemeijer<sup>1</sup>, J. Stedehouder<sup>1</sup>, B. Distel<sup>2,3,4</sup>, Y.  
Elgersma<sup>2,3</sup>, F.M.S. de Vrij<sup>1</sup>, S.A. Kushner<sup>1,3</sup>

<sup>1</sup>Dept of Psychiatry, Erasmus MC, Wytemaweg 80, 3015 CN Rotterdam, The Netherlands

<sup>2</sup>Dept of Neuroscience, Erasmus MC, Wytemaweg 80, 3015 CN Rotterdam, The Netherlands

<sup>3</sup>ENCORE Expertise Center for Neurodevelopmental Disorders, Erasmus MC University Medical Center, Rotterdam, 3015 CN, The Netherlands

<sup>4</sup>Department of Medical Biochemistry, Amsterdam UMC, University of Amsterdam, Amsterdam, 1105AZ, The Netherlands

<sup>§</sup>Both authors contributed equally to this work

Manuscript in preparation

## ABSTRACT

Maternal loss of functional UBE3A protein causes the neurodevelopmental disease Angelman Syndrome (AS). Despite the identification of the causative gene (*UBE3A*), the precise function of UBE3A in the pathophysiology of AS remains unknown. In mice, three *Ube3a* transcriptional isoforms have been reported, of which two appear to be translated (mouse UBE3A protein isoform 2 and 3). Mouse UBE3A protein isoform 2 is predominantly localized to the cytoplasm, while mouse UBE3A protein isoform 3 is almost exclusively nuclear. In contrast, little is known about the localization of human UBE3A. Using human post-mortem tissue lysates, we examined the expression of UBE3A protein isoforms. We find at least two different UBE3A protein isoforms, which most likely correspond to human UBE3A protein isoform 1 (ortholog of mouse UBE3A protein isoform 3) and human UBE3A protein isoform 2 (no mouse ortholog) and/or human UBE3A protein isoform 3 (ortholog of mouse UBE3A protein isoform 2). To examine potential differences in UBE3A between mouse and human, we examined the localization of transiently transfected mouse and human UBE3A protein isoforms in UBE3A-null mouse hippocampal neurons and human neurons derived from induced pluripotent stem cells. We found that mouse UBE3A isoform 3 and human ortholog UBE3A isoform 1 have a predominantly nuclear localization in both mouse and human neurons. Conversely, mouse UBE3A isoform 2 has a predominantly cytoplasmic localization in both mouse and human neurons. Notably however, human UBE3A isoform 3, the ortholog of mouse UBE3A isoform 2, has a predominantly nuclear localization in both mouse and human neurons. Taken together, we conclude that the mouse versus human cellular context does not appear to be a critical modulator of the distinct cytoplasmic or nuclear localization of the various UBE3A isoforms. Rather, the highly distinct localizations of the orthologous mouse UBE3A isoform 2 and human UBE3A isoform 3 is likely a result from the few differences in their protein sequences.

## INTRODUCTION

In 1997, genetic abnormalities of maternally inherited *UBE3A* were established to cause Angelman Syndrome (AS)<sup>1,2</sup>, a rare neurodevelopmental disease that affects between 1:15.000 – 1:30.000 children. Children with AS exhibit a range of neurodevelopmental impairments, including severe intellectual disability, movement and balance problems, happy demeanor and absence of speech<sup>3</sup>. The *UBE3A* gene is parentally imprinted. In nearly all expressing cell types it is transcribed bi-allelically. In neurons, however, *UBE3A* expression occurs almost exclusively from the maternal allele, while the paternal allele is silenced by a long non-coding RNA transcript (*UBE3A-ATS*)<sup>4-7</sup>. The protein product of the *UBE3A* gene is a HECT domain ubiquitin E3 ligase, which functions to target proteins for proteasomal degradation<sup>8,9</sup>. Although several cytoplasmic and nuclear targets of *UBE3A*-mediated ubiquitination have been proposed<sup>8-10</sup>, very few have been confirmed, leaving a major open question regarding how lack of functional *UBE3A* causes Angelman Syndrome.

*UBE3A* has mostly been studied in mice. In mouse neurons, *UBE3A* is weakly localized to synapses, dendrites, endoplasmic reticulum, and mitochondria, while the nuclear localization is particularly high<sup>11-14</sup>. *UBE3A* localization appears dependent on developmental age. Immature neurons exhibit moderate *UBE3A* expression within both the cytoplasm and nucleus, while *UBE3A* expression in mature neurons is predominantly nuclear<sup>11,13,14</sup>.

AS mouse models replicate many of the core features of AS, including motor dysfunction, inducible epilepsy, learning deficiencies, anxiety- and autism-related phenotypes and repetitive behavior<sup>15-19</sup>. Anxiety- and autism-related phenotypes, as well as repetitive behavior and epilepsy, can be rescued when *Ube3a* expression is re-established before 3 weeks of age<sup>17</sup>. As such, *Ube3a* appears essential in early development. Since *UBE3A* localization is age-dependent and its expression is crucial in development, *UBE3A*'s cellular localization could reveal mechanistic details about its involvement in disease pathology.

Mice express three different *Ube3a* isoforms<sup>11,20</sup>. Mouse *UBE3A* isoforms 2 and 3 differ only in a 21-amino-acid N-terminus. Mouse *UBE3A* isoform 1 resembles isoform 3, however misses a large part of the catalytic HECT-domain at the C-terminus (**Figure 1**). Mouse *UBE3A* isoform 2 resides mostly in the cytoplasm in HEK293 cells and primary mouse neurons<sup>11,20</sup>. In contrast, the localization of mouse *UBE3A* isoform 3 is predominantly nuclear<sup>11,20</sup>. Mouse isoform 1 has functions at RNA level<sup>21</sup>. The human *UBE3A* gene contains three open-reading frames, corresponding to three different *UBE3A* protein isoforms<sup>22</sup>. Human *UBE3A* isoform 1 and 3 show high amino-acid similarity to mouse *UBE3A* isoform 3 and 2 respectively (**Figure 1**), yet so far human *UBE3A* isoform expression and function has not been investigated. Human *UBE3A* isoform 2 does not have a mouse orthologue, and its existence remains to be empirically determined. *UBE3A-005* (ENST00000604860), an *in silico* predicted human transcript, mostly resembles mouse *UBE3A* isoform 1.

In this study, we use human post-mortem tissue and neural cultures derived from human induced pluripotent stem (iPSCs) cells to investigate the expression of human UBE3A. We find that human neurons express at least two different UBE3A protein isoforms, similar to mice. However, we also find that although mouse UBE3A isoform 2 and human UBE3A isoform 3 share high amino-acid homology, their localization is strongly divergent, suggesting distinct functions for human *UBE3A*.

## MATERIALS AND METHODS

### Cell Culture

Female *Ube3a*<sup>tm1Alb</sup> (*Ube3a*<sup>m+/p-</sup>) mice in the 129 background were crossed with wildtype B6 males and primary hippocampal neurons were isolated from the *Ube3A*<sup>m-/p+</sup> pups at E18 according Banker and Goslin<sup>23</sup>. All animal procedures were approved by a Dutch Ethical Committee for animal experiments. Primary skin fibroblasts were obtained from a 39-year-old female AS patient carrying a point mutation of *UBE3A* (c.1730G>A, p.W577X). The donor's caregiver provided written informed consent in accordance with the Medical Ethical Committee of the Erasmus University Medical Center. Stem cells were derived from fibroblasts as described previously using a single, multicistronic lentiviral vector encoding *OCT4*, *SOX2*, *KLF4* and *MYC*<sup>24</sup>. Quality control of iPS clones was performed by karyotyping, real-time quantitative PCR and embryonic body (EB) differentiation. Derivation and quality control of Ctrl line (Line 2<sup>25</sup>) as well as neuronal differentiation was previously described by Gunhanlar et al<sup>25</sup>. Neural precursors cells (NPCs) were generated using an EB stage to induce neuroectoderm<sup>25</sup>. Resulting NPCs were sorted using a serial gating strategy using multiple markers to obtain a homogeneous population of forebrain-specific NPCs<sup>26</sup>. In short, NPCs at passage 3-5 were detached with accutase for 2 min at 37°C, collected and washed using PBS+2% serum. Cells were resuspended in 100-200 µl PBS+2% serum and stained on ice for 30 min with 1:100 CD15 V450 (561584, BD Bioscience), 1:250 CD24 PE-Cy7 (561646, BD Bioscience), 1:100 CD44 FITC (560977, BD Bioscience), 1:250 CD184 APC (560936, BD Bioscience), and 1:500 CD271 PE (560927, BD Bioscience)<sup>26</sup>. After staining, cells were washed twice using PBS+2% serum. Stained cells were passed through a 100 µm filter and sorted on a FACS Aria III (BD Biosciences). CD184+/CD44-/CD271-/CD24+ cells were collected in laminin-coated plates and expanded in NPC medium<sup>25</sup>. The WTC-11 NPC line (Gladstone Institute) was used as a Ctrl to compare AS-derived NPCs to. To obtain human neurons, NPCs were plated on polyornithine/laminin-coated coverslips in neuronal differentiation medium<sup>25</sup>. After 4 weeks of differentiation, only half of the medium of the cultures was replenished. Neuronal cultures were differentiated for 3-12 weeks.

## Western blot

To generate lysates for western blot, cortex of adult mice (n=3, 10-12 weeks old) and fresh-frozen human postmortem tissue blocks of three subjects (table 1) were treated as described in Wang et al<sup>27</sup>. A total of 20 ug of each sample was loaded on the gel and a wet transfer was performed. The blotted nitrocellulose membrane was probed with antibodies directed against UBE3A (E8655, Sigma–Aldrich; 1:1,000) and Actin (MAB1501R, Millipore; 1:20,000). A fluorophore-conjugated secondary goat anti-mouse antibody (IRDye 800CW, Westburg; 1:15,000) was used and the protein was detected using Li-cor Odyssey Scanner system.

**Table 1**, Demographics human postmortem tissue for western blot analysis and immunohistochemistry

Experiment	Gender	Age	Region
1 Western blot	male	66	Right superior frontal gyrus
2 Western blot	female	58	Left superior frontal gyrus
3 Western blot	male	50	Left superior frontal gyrus
4 Immunohistochemistry	female	61	Left superior temporal gyrus
5 Immunohistochemistry	male	79	Left superior temporal gyrus

## Human brain immunohistochemistry

Left superior temporal gyrus tissue blocks of two subjects were obtained from the pathology department of Erasmus MC and stored at -80°C (table 1). These samples were fixed for 3 days in 4% paraformaldehyde (0.1M phosphate buffer, pH 7.3) at 4°C. Tissue was subsequently transferred to 10% sucrose (0.1M phosphate buffer, pH 7.3) overnight at 4°C, and stored in 30% sucrose (0.1M phosphate buffer, pH 7.3) for a maximum of 7 days at 4°C. Serial 40 µm sections were collected perpendicular to the cortical surface using a freezing microtome (Leica, Wetzlar, Germany; SM 2000 R) and stored at 4°C in 0.1M phosphate buffer for a maximum of 7 days. Free-floating sections were washed with PBS at room temperature preceding pre-incubation. Sections were pre-incubated with a blocking PBS buffer containing 0.5% Triton X-100 and 5% bovine serum albumin (BSA) for 1h at room temperature. Primary antibody labeling was performed in PBS buffer containing 0.5% Triton X-100 and 1% BSA for 72h at 4°C. The following primary antibodies were used: Mouse anti-UBE3A (SAB1404508, Sigma; 1:150), and rabbit anti-MAP2 (AB5622, Millipore; 1:300). Following primary antibody labeling, sections were washed with PBS and incubated with the following secondary antibodies: Alexa-488 anti-rabbit and Cy3 anti-mouse (Jackson ImmunoResearch; 1:200) in PBS buffer containing 0.5% Triton X-100, 1% BSA for 6 h at room temperature. Nuclear staining was performed using DAPI (1:10,000, Thermo Fisher Scientific, Waltham, MA, USA) in 0.1M phosphate buffer for 1h. Subsequently, sections were washed twice in 0.1M phosphate buffer, submerged in chromalin solution and mounted using Vectashield antifade medium. Images were acquired using a Zeiss LSM 700 confocal microscope (Carl Zeiss, Oberkochen, Germany).

### Plasmid DNA constructs and cloning

Mouse Ube3A constructs were amplified from mouse cDNA using a combination of forward and reverse primers introducing AscI and PacI restriction sites at the 5' and 3' end of the gene fragments respectively. Human UBE3A constructs were amplified from the p4053 HA-E6AP isoform1 (Addgene #8657) and p4055 HA-E6AP isoform III (Addgene #8659) using a combination of forward and reverse primers introducing AscI and NotI sites at the 5' and 3' end of the gene fragment respectively. PCR products were cloned by A-tailing into pGEMTeasy (Promega) and sequenced. PCR products were then cloned in the dual promoter vector CAGG-tdTomato (Clontech) described in Kury et al.<sup>28</sup>. To prohibit production of protein products of the second in-frame methionine in the mouse UBE3A isoform 2 and human UBE3A isoform 3 constructs, the methionine was replaced with an alanine (M22A, M21A, respectively).

### Transfections in mouse and human neurons

Primary mouse hippocampal neurons were transfected after 7 days *in vitro* (DIV) with one of the mouse or human UBE3A constructs (in total 1.8 µg DNA per 12-well coverslip). Lipofectamine 2000 was used to transfect neurons, according to the manufacturer's instructions (Invitrogen). Neurons were fixed 4 days post-transfection with 4% paraformaldehyde (PFA)/4% sucrose and stained for UBE3A and MAP2. The following primary antibodies were used: anti-MAP2 (188004, Synaptic Systems; 1:500) and anti-UBE3A (SAB1404508, Sigma; 1:200). Human neurons were differentiated for 3 weeks and transfected with 2 µg DNA per 12-well coverslip, using Lipofectamine 3000 (Invitrogen) according manufacturer's protocol. Three days post-transfections human neurons were fixed and stained using 4% formaldehyde in phosphate-buffered saline. Primary antibodies were incubated overnight at 4 °C in labeling buffer containing 0.05M Tris, 0.9% NaCl, 0.25% gelatin and 0.5% Triton-X-100 (pH 7.4). The following primary antibodies were used: anti-MAP2 (188004, Synaptic Systems; 1:200) and anti-UBE3A (SAB1404508, Sigma; 1:200) The following secondary antibodies were used: Alexa-488 anti-guinea pig and Cy3 anti-mouse (Jackson ImmunoResearch; 1:200). Samples were imbedded in Mowiol 4-88 (Sigma-Aldrich), after which confocal imaging was performed with a Zeiss LSM700 confocal microscope using ZEN software (Zeiss, Oberkochen, Germany). Of each condition 12-15 transfected cells were examined.

## RESULTS

### UBE3A isoform expression in human brain

Mouse *Ube3a* and human *UBE3A* both contain open-reading frames for three different E3 ubiquitin ligase protein (UBE3A) isoforms (**Figure 1**). These isoforms are indicated as mouse isoform 1 (NM\_173010), 2 (NM\_011668) and 3 (NM\_001033962) and human isoform 1

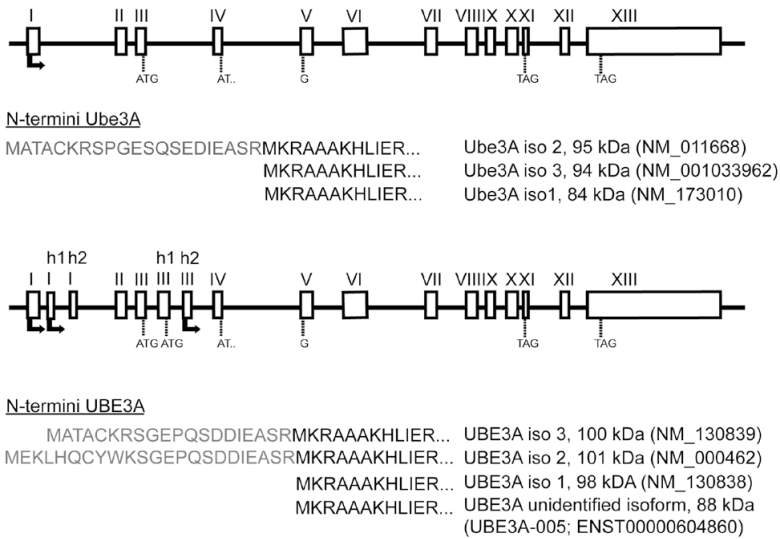
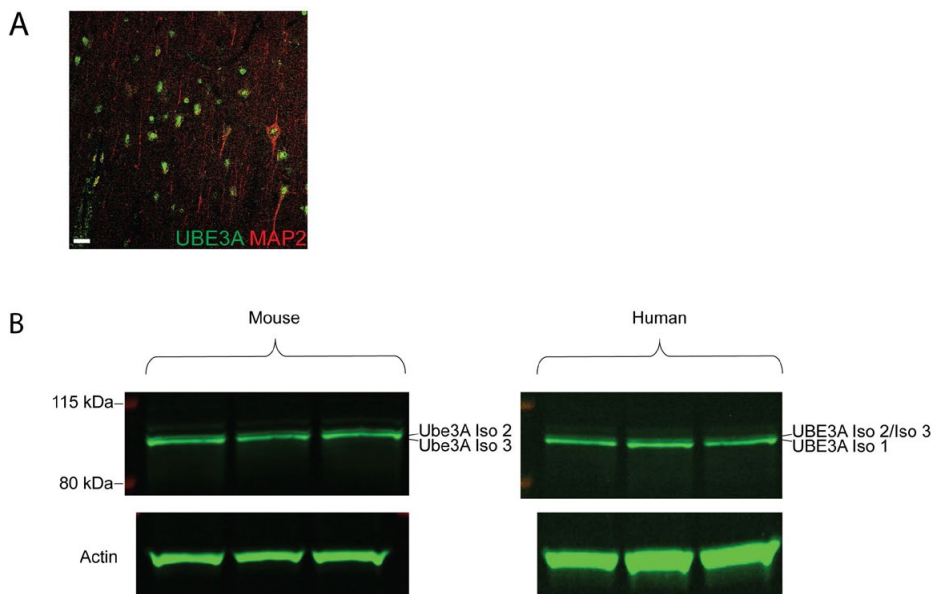


Figure 1. Mouse *UBE3A* and human *UBE3A* gene structure and protein isoforms

(NM\_130838), 2 (NM\_000462) and 3 (NM\_130839)<sup>22</sup>. Mouse *UBE3A* isoform 2 is orthologous to human *UBE3A* isoform 3 (96% identity in amino acid sequence). Mouse *UBE3A* isoform 3 is orthologous to human *UBE3A* isoform 1 (96% identity in amino acid sequence). Human *UBE3A* isoform 2 does not have a mouse orthologue, due to the usage of a human-specific promoter. Mouse *UBE3A* isoform 1 mostly resembles UBE3A-005, ENST00000604860, an *in silico* predicted transcript, which has not yet been confirmed experimentally. Similarly, mouse *UBE3A* isoform 1 protein has also not been confirmed experimentally, though RNA functionality has been reported<sup>21</sup>.

Mouse *UBE3A* protein localization and expression has been extensively studied<sup>11,12,29</sup>, however human *UBE3A* protein localization and expression remains poorly characterized. We therefore stained human post-mortem brain slices (superior temporal gyrus, n=2 different individuals) for *UBE3A* expression. We found *UBE3A* predominantly in the nucleus (Figure 2A), comparable to mouse *UBE3A*<sup>12-14</sup>. We did not observe *UBE3A* staining in astrocytes.

Given the importance of confirming the translatability of mouse *UBE3A* biology for understanding the pathophysiology of human *UBE3A* mutations in Angelman Syndrome, we assessed the isoform-specific expression of *UBE3A* in post-mortem human cortex. Figure 2B shows a western blot of lysates of three adult mouse and three adult human post-mortem cerebral cortex samples. We found that, comparable to mice, human cerebral cortex lysates contain two protein isoforms. Considering the open reading frames of *UBE3A*, these isoforms most likely correspond to human *UBE3A* isoform 1 and human *UBE3A* isoform 2 and/or isoform 3, given that the latter two would be indistinguishable by size. Human *UBE3A* isoform 1 and mouse *UBE3A* isoform 3 are the most abundant protein isoforms in each species.



**Figure 2. Two UBE3A protein isoforms discernible in mouse and human brain.** (A) Immunohistochemical labeling of UBE3A and MAP2 in human superior temporal gyrus showing prominent nuclear labeling of UBE3A in neurons. Scale bar 20  $\mu\text{m}$ . (B) Western blot analysis of UBE3A protein in WT mouse brain and post-mortem human brain samples. Each lane represents one test animal or human subject. The bands ca. 100 kDa represent the different UBE3A protein isoforms.

### Human neurons derived from induced pluripotent stem cells recapitulate UBE3A localization from cerebral cortex

In order to examine human neurodevelopmental *UBE3A* expression and subcellular localization, we utilized human iPSC-derived neural precursor cells (NPCs) and neurons that were differentiated for successively longer intervals<sup>25</sup>. In control NPCs, UBE3A was distributed throughout both the cytoplasm and nucleus, whereas in neurons UBE3A was predominantly localized to the nucleus with minimal cytoplasmic labeling (**Figure 3A,B**), consistent with previous studies in mice<sup>11,13,14</sup> and our findings in human post-mortem tissue. No discernible UBE3A labeling was observed in dendrites, synapses, or in astrocytes.

We also generated iPSC-derived neuronal lineage cells from an AS patient carrying a point mutation (c.1730 G>A, p.W577X) resulting in a premature stop codon in the HECT-domain of UBE3A. Whereas UBE3A localization was similar to controls in NPCs (**Figure 3A**), *UBE3A* expression was undetectable in AS patient-derived neurons differentiated for 3, 6, 9 or 12 weeks (**Figure 3B**). Taken together, these findings confirm that human iPSC-derived neuronal lineage cells retain the imprinting mechanism governing *UBE3A* paternal allele silencing specifically during neurogenesis, and faithfully models the cell-type specific localization of UBE3A protein observed in human brain tissue.



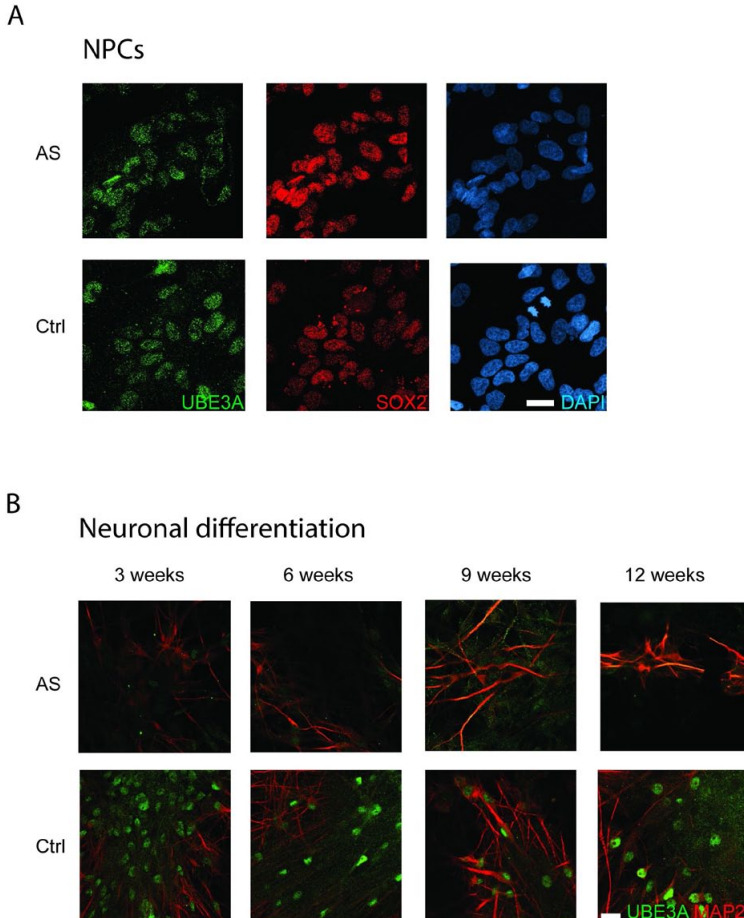


**Figure 3. Nuclear localization of UBE3A in Ctrl iPSC-derived neurons but no UBE3A in AS iPSC-derived neurons.** (A) Immunocytochemical labeling of UBE3A and neural progenitor marker SOX2 in Ctrl and AS NPCs (B) UBE3A and MAP2 labeling of 3-, 6-, 9- and 12-week-old human neurons derived from iPSCs from Ctrl subject and AS patient. Scale bar 20  $\mu$ m.

### Distinct subcellular localization of mouse UBE3A isoform 2 and the orthologous human UBE3A isoform 3

A previous study reported that mouse UBE3A isoforms 2 and 3 are predominantly localized to the cytoplasm and nucleus, respectively in both HEK293 cells and neurons<sup>11,20</sup>. We asked whether the orthologous human UBE3A isoforms exhibit a similar subcellular localization. We transfected primary hippocampal neurons from *Ube3a* knockout mice to assess isoform-specific localization in a *UBE3A* null background. As expected, mouse UBE3A isoform 2 was predominantly localized to the cytoplasm, while mouse UBE3A isoform 3 was localized to the nucleus (**Figure 4A**). The human ortholog of mouse UBE3A isoform 3, human UBE3A isoform 1, similarly was predominantly localized in the nucleus. However, human UBE3A

isoform 3 was also predominantly found in the nucleus, making its localization highly distinct from the cytoplasmic localization of its ortholog mouse UBE3A isoform 2 (**Figure 4A**).

We next considered whether the discordant localization between human UBE3A isoform 3 and its orthologue mouse UBE3A isoform 2 resulted from *cis*- or *trans*-acting factors. In particular, we considered whether the localization of human UBE3A isoform 3 might be different in mouse versus human neurons. Therefore, we individually expressed the mouse and human isoforms in human AS patient (*UBE3A* null) iPSC-derived neurons (**Figure 4B**). Mouse isoform 2 was consistently found in the cytoplasm and mouse isoform 3 was localized to the nucleus when expressed in human neurons, consistent with their respective localization in mouse neurons. Moreover, both human isoform 3 and human isoform 1 were constantly found in the nucleus, again consistent with their localization in mouse neurons. Therefore, the distinct localization of mouse UBE3A isoform 2 (cytoplasmic) and orthologous human UBE3A isoform 3 (nuclear) is likely due to a differential *cis*-acting mechanism within the protein itself.

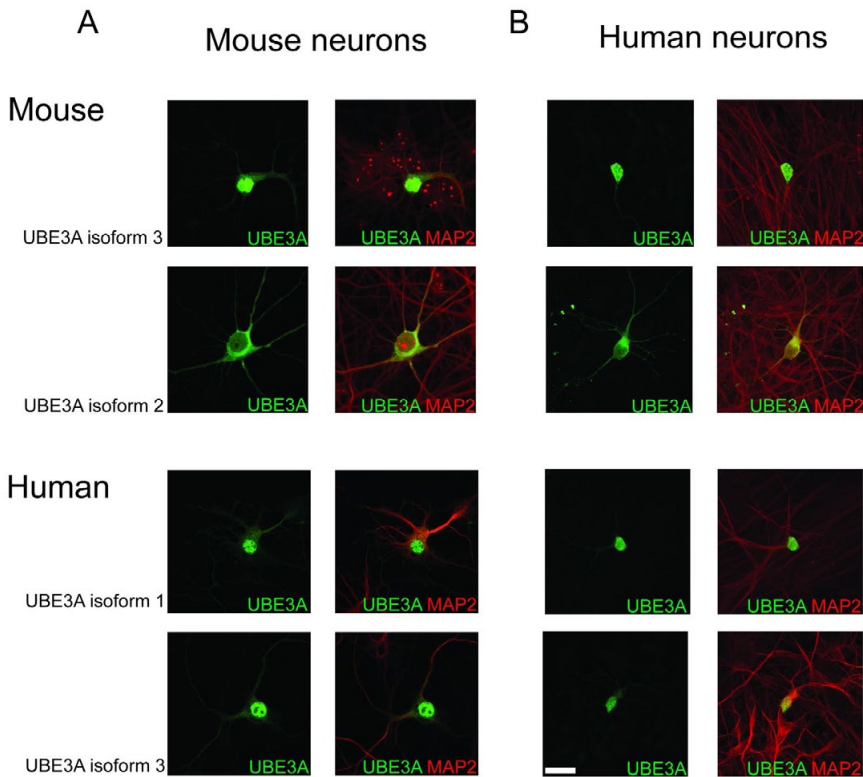


**Figure 4. Localization of mouse and human UBE3A protein isoforms in mouse and human neurons.** (A), (B) Representative immunocytochemical UBE3A and MAP2 stainings of (A) primary hippocampal neurons from AS mouse and (B) human neurons derived from iPSCs from AS patient transfected with constructs over-expressing indicated UBE3A protein isoforms. Scale bar 20  $\mu$ m.

## DISCUSSION

Loss of function of the maternal *UBE3A* gene is responsible for the neurodevelopmental disorder Angelman Syndrome<sup>1,2</sup>. Mice with a deletion of *Ube3a* show AS-related phenotypes and have served as a model to study UBE3A<sup>15,17,19,30</sup>. Given the high orthology between the protein-coding sequences of mouse and human UBE3A (96% protein sequence homology), it has widely been assumed that knowledge of the mouse UBE3A biology is valid for humans. Here we reveal a potentially important discordance between the subcellular localization of orthologous mouse and human UBE3A isoforms. The dissimilar localization suggests that the few differences between the mouse *Ube3a* and human *UBE3A* gene sequence might be the critical determinants of their distinct subcellular localization.

Analogous to mice<sup>11</sup>, humans express at least two major UBE3A protein isoforms in brain. In mature neurons of mice, UBE3A is predominantly localized to the nucleus<sup>11,13,14</sup>. Notably, using both post-mortem brain tissue and iPSC-derived neurons, we find a similar localization in human neurons. Prior studies have shown that in mice UBE3A localization is dynamic during brain development<sup>13,14</sup>: in immature neurons UBE3A is distributed broadly across the cytoplasm and nucleus, while in mature neurons it concentrates within the nucleus. The development of the cortical layers results in a transient simultaneous existence of mature and immature neurons<sup>14</sup>. As AS symptoms emerge in the early postnatal period, a spatiotemporal expression analysis of early neurodevelopmental human *UBE3A* expression may provide the opportunity to elucidate the early neurodevelopmental processes in which UBE3A is indispensable.

Our western blot data shows the expression of at least two UBE3A isoforms. Similarly, we replicated earlier reports of two mouse UBE3A isoforms, mouse UBE3A isoform 2 and isoform 3, which constitute approximately 75-80% and 20-25% of total UBE3A protein, respectively<sup>20</sup>. Human UBE3A isoform expression ratios are similar<sup>20</sup>, yet we cannot specify the contribution of the different human isoform 2 and 3 as they are indistinguishable on a western blot. Unfortunately the lack of isoform-specific antibodies for mouse or human UBE3A has frustrated attempts to examine the relative expression and localization of the various isoforms *in situ*. However, in lieu of isoform-specific antibodies, we individually expressed the mouse and human UBE3A isoforms in primary mouse neurons or iPSC-derived neurons lacking maternal UBE3A expression.

For over 15 years, several AS mouse models have been used to study AS<sup>15-17,19</sup>. On the basis of the high homology between the mouse and human UBE3A protein sequence, mice have traditionally been assumed to be sufficient for studying UBE3A neurobiology and the pathophysiology of AS. Notably however, we have now discovered a major difference in the subcellular localization of mouse isoform 2, which is predominantly cytoplasmic<sup>11,20</sup>, and the orthologous human isoform 3, which is predominantly nuclear. Importantly, we observed the same differential pattern of subcellular localization in both primary mouse neurons and hu-

man iPSC-derived neurons, excluding species-specific *trans*-acting factors as the underlying cause. Therefore, we conclude that the few differences in their protein sequence are likely to be the critical determinants of their differential subcellular localization. In particular, an intriguing candidate region is the N-terminus of the protein, which has been shown by Trezza et al.<sup>20</sup> to robustly determine the subcellular localization of UBE3A. Compared to mouse isoform 2, the N-terminus of human isoform 3 contains differences at three amino acid positions:  $\Delta$ P9, S12P, and E15D (**Figure 1**). As the latter comprises a conservative amino acid change between acidic residues, this substitution may not have a strong effect on protein function. In contrast, the  $\Delta$ P9 and S12P substitution are particularly notable candidates that could influence dissimilar localization.

What the function of alternatively localized human UBE3A protein is, remains to be seen. In mice, several substrates in cytoplasm and nucleus have been proposed, but few have been independently confirmed<sup>8-10</sup>. Also, a previous report suggested that UBE3A functions as a nuclear co-transcriptional activator<sup>31</sup>. Notably, both human and mouse UBE3A contain a zinc-finger domain, which may mediate RNA, DNA and/or protein interactions. Since the majority of studies have been performed in mice, independent validation in human neurons remains necessary. Additionally, a recent report has proposed that the subcellular localization of UBE3A may be further regulated by neuronal activity<sup>32</sup>, a possibility that requires further mechanistic investigation.

In our experiments we did not detect UBE3A in astrocytes, yet other studies have reported some limited expression of *UBE3A* in glial cells<sup>13,14</sup>. Notably however, UBE3A isoform-specific subcellular localization has remained largely unexplored in glial cells, leaving open the possibility of an unrecognized function of UBE3A in glial cells.

The function of the individual UBE3A isoforms remains poorly understood. In mice, UBE3A isoform 2 rescued impaired dendrite polarity in neurons with knock-down of *Ube3A*<sup>11</sup>. The function of mouse isoform 3 is unknown, yet its RNA is increased with neural activity<sup>32</sup>. A recent study shows that in mice with isoform-specific deletions, AS phenotypes were recapitulated in mice lacking isoform 3, whereas mice lacking isoform 2 were phenotypically comparable to wild types<sup>20</sup>. Analogously in humans, Sathwani et al. reported an AS patient with a T>C variant point mutation in the start-codon of human UBE3A isoform 1 (ortholog of mouse isoform 3) that causes AS<sup>33</sup>. This mutation is predicted to abrogate translation of UBE3A isoform 1, but also introduces a methionine to threonine substitution in both human UBE3A isoform 2 and 3. Accordingly, it cannot be excluded that the altered or compensatory function of the remaining UBE3A isoform 2 and/or 3 are also contributing to the phenotype.

With the advent of human iPSC technology, the study of human neurobiology has become more tractable. Several groups have utilized iPSCs to investigate AS pathophysiology<sup>34,35</sup>. Previous models demonstrated several molecular characteristics of *UBE3A* biology, including imprinting and allele-specific silencing<sup>7,34</sup>. A recent study also reported electrophysiological alterations in neurons derived from iPSCs of AS patients<sup>35</sup>. Our findings from AS patient

iPSC-derived neurons are also consistent with imprinting and allele-specific silencing. iPSC-derived NPCs were UBE3A positive, despite a nonsense mutation in the maternal *UBE3A*, consistent with bi-allelic expression. In contrast, in iPSC-derived neurons no UBE3A was detected following just 3 weeks of differentiation from NPCs, as would be expected following paternal allele silencing in cells harboring a nonsense mutation in maternal *UBE3A*.

Trezza et al. highlight the importance of nuclear UBE3A for proper neurodevelopment<sup>20</sup>. As our iPSC-derived neural cultures likely reflect late gestational or early postnatal neurons<sup>25</sup>, it is possible that human UBE3A may localize to the nucleus prenatally. As such, investigation of the early neurodevelopmental subcellular localization in human neurons may also be important for understanding AS pathophysiology and identifying efficacious therapeutic interventions.

## REFERENCES

1. Kishino, T., Lalande, M. & Wagstaff, J. UBE3A/E6-AP mutations cause Angelman syndrome. *Nat. Genet.* **15**, (1997).
2. Matsuura, T. *et al.* De novo truncating mutations in E6-AP ubiquitin-protein ligase gene (UBE3A) in Angelman syndrome. *Nat. Genet.* **15**, (1997).
3. Williams, C. A., Beaudet, A. L. & Clayton-Smith, Ji. Angelman syndrome 2005: updated consensus for diagnostic criteria. *Am. J. Med. Genet. A* **140A**, 413–418 (2006).
4. Rougeulle, C., Glatt, H. & Lalande, M. The Angelman syndrome candidate gene, UBE3A/E6-AP, is imprinted in brain. *Nat. Genet.* **17**, (1997).
5. Rougeulle, C., Cardoso, C., Fontés, M., Colleaux, L. & Lalande, M. An imprinted antisense RNA overlaps UBE3A and second maternally expressed transcript. *Nat. Genet.* **19**, (1998).
6. Chamberlain, S. J. *et al.* Induced pluripotent stem cell models of the genomic imprinting disorders Angelman and Prader – Willi syndromes. *PNAS.* **107**:41, 17668–17673 (2010).
7. Martins-taylor, K. *et al.* Imprinted expression of UBE3A in non-neuronal cells from a Prader-Willi syndrome patient with an atypical deletion. *Human Mol Gen* 1–31 (2013).
8. Sell, G. L. & Margolis, S. S. From UBE3A to Angelman syndrome: A substrate perspective. *Front. Neurosci.* **9**, 1–6 (2015).
9. LaSalle, J. M., Reiter, L. T. & Chamberlain, S. J. Epigenetic regulation of UBE3A and roles in human neurodevelopmental disorders. *Epigenomics* **7**, 1213–28 (2015).
10. Mabb, A. M., Judson, M. C., Zylka, M. J. & Philpot, B. D. Angelman syndrome: insights into genomic imprinting and neurodevelopmental phenotypes. *Trends Neurosci.* **34**, 293–303 (2011).
11. Miao, S. *et al.* The Angelman Syndrome Protein Ube3a Is Required for Polarized Dendrite Morphogenesis in Pyramidal Neurons. *J. Neurosci.* **33**, 327–333 (2013).
12. Dindot, S. V., Antalffy, B. a., Bhattacharjee, M. B. & Beaudet, A. L. The Angelman syndrome ubiquitin ligase localizes to the synapse and nucleus, and maternal deficiency results in abnormal dendritic spine morphology. *Hum. Mol. Genet.* **17**, 111–118 (2008).
13. Burette, A. C. *et al.* Subcellular organization of UBE3A in neurons. *J. Comp. Neurol.* **00**, 1–19 (2016).
14. Judson, M. C., Sosa-Pagan, J. O., Del Cid, W. A., Han, J. E. & Philpot, B. D. Allelic specificity of Ube3a expression in the mouse brain during postnatal Development. *J. Comp. Neurol.* **522**, 1874–1896 (2014).
15. Jiang, Y. H. *et al.* Mutation of the Angelman ubiquitin ligase in mice causes increased cytoplasmic p53 and deficits of contextual learning and long-term potentiation. *Neuron* **21**, 799–811 (1998).
16. Meng, L. *et al.* Truncation of Ube3a-ATS Unsilences Paternal Ube3a and Ameliorates Behavioral Defects in the Angelman Syndrome Mouse Model. *PLoS Genet.* **9**, (2013).
17. Silva-santos, S. *et al.* Ube3a reinstatement identifies distinct developmental windows in a murine Angelman syndrome model. *J of Clinical Invest.* **125**, 1–8 (2015).
18. Huang, H. S. *et al.* Behavioral deficits in an Angelman syndrome model: Effects of genetic background and age. *Behav. Brain Res.* **243**, 79–90 (2013).
19. van Woerden, G. M. *et al.* Rescue of neurological deficits in a mouse model for Angelman syndrome by reduction of alphaCaMKII inhibitory phosphorylation. *Nat. Neurosci.* **10**, 280–2 (2007).
20. Rossella Trezza, A. *et al.* Loss of nuclear UBE3A causes electrophysiological and behavioral deficits in mice and is associated with Angelman syndrome. *Nat Neuroscience.* **22**(8):1235–1247 (2019)
21. Valluy, J. *et al.* A coding-independent function of an alternative Ube3a transcript during neuronal development. *Nat. Neurosci.* **18**, 666–673 (2015).
22. Yamamoto, Y., Huibregtse, J. M. & Howley, P. M. The human E6-AP gene (UBE3A) encodes three potential protein isoforms generated by differential splicing. *Genomics* **41**, 263–266 (1997).

23. Banker, G. & Goslin, K. *Culturing nerve cells*. Cambridge MA MIT Press (1991).
24. Warlich, E. *et al.* Lentiviral vector design and imaging approaches to visualize the early stages of cellular reprogramming. *Mol. Ther.* **19**, 782–9 (2011).
25. Gunhanlar, N. *et al.* A simplified protocol for differentiation of electrophysiologically mature neuronal networks from human induced pluripotent stem cells. *Mol. Psychiatry* 1–9 (2017). doi:10.1038/mp.2017.56
26. Yuan, S. H. *et al.* Cell-surface marker signatures for the Isolation of neural stem cells, glia and neurons derived from human pluripotent stem cells. *PLoS One* **6**, (2011).
27. Wang, T., van Woerden, G. M., Elgersma, Y. & Borst, J. G. G. Enhanced Transmission at the Calyx of Held Synapse in a Mouse Model for Angelman Syndrome. *Front. Cell. Neurosci.* **11**, 1–19 (2018).
28. Küry, S. *et al.* De Novo Mutations in Protein Kinase Genes CAMK2A and CAMK2B Cause Intellectual Disability. *Am. J. Hum. Genet.* **101**, 768–788 (2017).
29. Burette, A. C. The subcellular organization of UBE3A in neurons. *J. Comp. Neurol.* **520**, 633–655 (2011).
30. Meng, L., Person, R. E. & Beaudet, A. L. Ube3a-ATS is an atypical RNA polymerase II transcript that represses the paternal expression of Ube3a. *Hum. Mol. Genet.* **21**, 3001–3012 (2012).
31. Nawaz, Z. *et al.* The Angelman syndrome-associated protein, E6-AP, is a coactivator for the nuclear hormone receptor superfamily. *Mol. Cell. Biol.* **19**, 1182–1189 (1999).
32. Filonova, I., Trotter, J. H., Banko, J. L. & Weeber, E. J. Activity-dependent changes in MAPK activation in the Angelman Syndrome mouse model. *Learn. Mem.* **21**, 98–104 (2014).
33. Sadhwani, A. *et al.* Two Angelman families with unusually advanced neurodevelopment carry a start codon variant in the most highly expressed UBE3A isoform. *American J of Med Gen* 1–7 (2018).
34. Chamberlain, S. J. *et al.* Induced pluripotent stem cell models of the genomic imprinting disorders Angelman and Prader-Willi syndromes. *Proc. Natl. Acad. Sci. U. S. A.* **107**, 17668–73 (2010).
35. Fink, J. J. *et al.* Disrupted neuronal maturation in Angelman syndrome-derived induced pluripotent stem cells. *Nat. Commun.* **8**, 15038 (2017).